Publication P1

Seman, S., Niiranen, J., Kanerva, S., Arkkio, A. 2004. ”Analysis of a 1.7 MVA Doubly Fed Wind-Power Induction Generator during Power Systems Disturbances”. *Proceedings of NORPIE 2004*, 14-16 June 2004, Trondheim, Norway, 6 p., (CD-ROM), Available: http://www.elkraft.ntnu.no/norpie/10956873/Final%20Papers/046%20-%20NORP-Seman.pdf (7.5.2006).

Analysis of a 1.7 MVA Doubly Fed Wind-Power Induction Generator during Power Systems Disturbances

S. Seman, *Student Member, IEEE*, J. Niiranen, S. Kanerva, and A. Arkkio

***Abstract*— The performance of a 1.7 MVA wind-power doubly fed induction generator (DFIG) under network fault is studied using simulator developed in MATLAB-Simulink. The simulator consists of the DFIG analytical model, the detailed frequency converter model including passive crowbar protection, and model of the transformer. The rotor-side frequency converter is controlled by a modified direct torque control (DTC). Simulation results show the transient behavior of the doubly fed induction generator when a sudden voltage dip is introduced with and without the crowbar implemented.**

***Index Terms*— Wind power, doubly fed induction generator, DTC, crowbar.**

I. Introduction

THE doubly fed induction generator (DFIG) wind turbines are nowadays more widely used especially in large wind farms. The main reason for the popularity of the doubly fed wind induction generators connected to the national networks is their ability to supply power at constant voltage and frequency while the rotor speed varies. The DFIG concept also provides a possibility to control the overall system power factor. DFIG wind turbine utilizes a wound rotor induction machine while the rotor winding is supplied from frequency converter providing speed control together with terminal voltage and power factor control for the overall system.

A few years ago, most of the national network codes and standards did not require supporting the power system from wind turbine during the fault in the network. Due to increase of the number of wind turbines connected to the network, new network codes were issued prescribing how the wind generator has to support the network during power disturbances in the network. Therefore it is necessary to carry out accurate transient simulations in order to understand the impact of the system disturbances on wind turbine. The transient simulation analysis is also a useful tool for the design of the rotor over-current protection. The over-current protection circuit, so called crowbar is needed in order to protect the rotor side frequency converter during disturbances in the network [1].

The most common approach in dynamic modeling of DFIG for wind turbines is using a space vector theory based model of a slip-ring induction machine [1]-[5]. This method provides sufficient accuracy also in case when the voltage dips due to one or two phase faults in the network [6] are studied. More advanced transient analysis when effect of magnetic saturation and skin effect in the rotor winding are taken into account would require another model of DFIG for example Finite Element Method model [7].

The transient analyses of the of the DFIG wind-turbine have been studied in [8] where the crowbar is realized by using of six anti-parallel thyristors and with an active crowbar in [9].

This paper presents the transient simulation analysis of a 2 MVA DFIG for wind power application under a three-phase network short circuit. The DFIG is simulated by means of space vector theory based analytical model of a slip-ring induction machine together with frequency converter, transformer and control in MATLAB - Simulink. The rotor-side frequency converter is controlled by modified DTC control strategy and a passive crowbar is connected between the rotor and rotor-side inverter as it is depicted in Figure 1. Simulation results show the transient behavior of the doubly fed induction generator when the sudden voltage dip is introduced with and without the crowbar implemented.

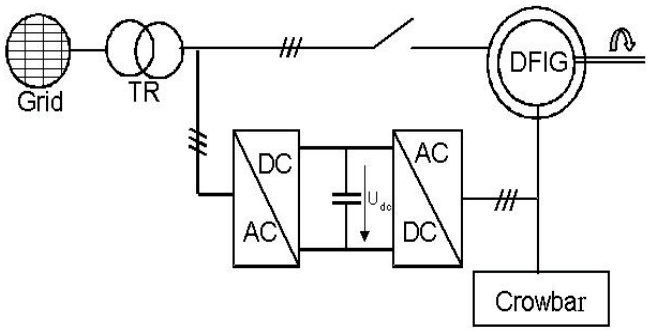

Fig. 1. Doubly fed wind-power induction generator with the crowbar.

This work was supported in part by the Tekniikan edistämissäätiö and the Fortumin säätio.

S. Seman, is with the Laboratory of Electromechanics, Helsinki University of Technology, P.O.Box 3000, FIN-02015 HUT, Finland (tel. +358 9 4512389, fax. +358 9 451 2991, e-mail: slavomir.seman@hut.fi).

J Niiranen, is with ABB Oy, P.O. Box 184, FIN-00381, Helsinki, Finland, (e-mail: jouko.niiranen@fi.abb.com)

S. Kanerva and A. Arkkio, are with the Laboratory of Electromechanics, Helsinki University of Technology, P.O. Box 3000, FIN-02015 HUT, Finland (e-mail: sami.kanerva@hut.fi, and antero.arkkio@hut.fi).

II. Model of the Doubly Fed Induction Generator

The machine equations written in a x-y reference frame fixed with rotor are:

$$\frac{d\psi_{s\_x}}{dt} = \sigma_S \left(\frac{L_r}{L_m}\psi_{s\_x} - \psi_{r\_x} \right) - p\omega_r \psi_{s\_x} + v_{s\_y} \quad (1)$$

$$\frac{d\psi_{s\_y}}{dt} = \sigma_S \left(\frac{L_r}{L_m}\psi_{s\_y} - \psi_{r\_y} \right) - p\omega_r \psi_{s\_y} + v_{s\_x} \quad (2)$$

$$\frac{d\psi_{r\_x}}{dt} = \sigma_R \left(\psi_{r\_x} - \frac{L_m}{L_s}\psi_{s\_x} \right) + v_{r\_x} \quad (3)$$

$$\frac{d\psi_{r\_y}}{dt} = \sigma_R \left(\psi_{r\_y} - \frac{L_m}{L_s}\psi_{s\_y} \right) + v_{r\_y} \quad (4)$$

Where:

$$\sigma_S = \frac{R_s L_m}{L_m L_m - L_s L_r},\ \sigma_R = \frac{R_r L_s}{L_m L_m - L_s L_r}$$

$$i_{s\_x} = \frac{L_m}{L_m L_m - L_s L_r}\left(\psi_{r\_x} - \frac{L_r}{L_m}\psi_{s\_x} \right) \quad (5)$$

$$i_{s\_y} = \frac{L_m}{L_m L_m - L_s L_r}\left(\psi_{r\_y} - \frac{L_r}{L_m}\psi_{s\_y} \right) \quad (6)$$

$$i_{r\_x} = \frac{L_s}{L_m L_m - L_s L_r}\left(\frac{L_m}{L_s}\psi_{s\_x} - \psi_{r\_x} \right) \quad (7)$$

$$i_{r\_y} = \frac{L_s}{L_m L_m - L_s L_r}\left(\frac{L_m}{L_s}\psi_{s\_y} - \psi_{r\_y} \right) \quad (8)$$

$$T_e = \frac{3}{2} p \left(\psi_{s\_y} i_{s\_x} - \psi_{s\_x} i_{s\_y} \right) \quad (9)$$

The symbols i_s, i_r denote the stator and rotor currents, respectively, v_s, v_r stator and rotor voltages and ψ_s, ψ_r stator and rotor flux linkages in two axis rotational (x-y) reference frame. R_s, R_r are stator and rotor resistance and L_s, L_r, L_m are stator, rotor inductances and magnetising inductance, respectively. The rotor speed is denoted as ω_r. Symbol p represents the number of pole-pairs, and T_e is the electromagnetic torque. The rated parameters are given in Table 1.

TABLE I
Ratings of the Generator

P_N	rated power	1.7 MVA
$U_{N,\ stator}$	rated stator voltage (line to line)	690 V (delta)
$U_{m,\ rotor}$	maximum rotor voltage	2472 V (star)
n_N	nominal speed	1500 rpm
$f_{N,\ stator}$	rated stator frequency	50 Hz

III. Frequency Converter And Control

The Frequency converter that supplies the rotor of DFIG consists of two back-to-back connected voltage source inverters (VSI).

A. Network Side Converter

The stator-side converter is represented in simulation by a discrete transfer function

$$H(z) = \frac{1}{1 + \tau_s z^{-1}} \quad (10)$$

where τ_s denotes the time constant of the first order discrete filter. The aim of the control of the stator side inverter is to supply the DC link and to maintain the level of dc-link voltage U_{dc} on a pre-set value. U_{dc} is controled by PI controller based algorithm.

B. Rotor Side Converter

The rotor side converter is supplied from a common DC-link and the switches are assumed to be ideal. The control of the rotor side frequency converter is realized by modified DTC strategy [10] as it is depicted in Fig. 2.

The magnitude of the rotor flux estimate $|\hat{\psi}_r|$ is calculated by means of Torque and Flux calculator from the measured rotor currents i_{ra}, i_{rb}, as

$$|\hat{\psi}_r| = \sqrt{(\hat{\psi}_{r\_x})^2 + (\hat{\psi}_{r\_y})^2} \quad (11)$$

where symbols $\hat{\psi}_{r\_x}$ and $\hat{\psi}_{r\_y}$ denote the estimated rotor fluxes in the two axis reference frame fixed to the rotor. The rotor flux estimates are

$$\hat{\psi}_{r\_x} = L_r i_{rx} + L_m i_{sx\_r} \quad (12)$$

$$\hat{\psi}_{r\_x} = L_r i_{ry} + L_m i_{sy\_r} \quad (13)$$

where i_{rx}, i_{ry} denote the rotor current components in the two-axis rotational reference frame and i_{sx_r}, i_{sy_r} denote the stator currents in the same frame.

The magnitude of the grid flux estimate $|\hat{\psi}_{grid}|$ that is used in control for synchronisation of DFIG with network is also calculated in Torque and Flux estimator from the measured stator currents i_{sA}, i_{sB} and stator voltages v_{sA}, v_{sB}.

The estimate of electromagnetic torque that is an input of the three-level hysteresis comparator is given by

$$\hat{T}_e = \frac{3}{2} p \left(i_{sx\_s}\psi_{sy\_s} - i_{sy\_s}\psi_{sx\_s} \right) \quad (14)$$

The reference values of the electromagnetic torque T_{e_ref} as well as rotational speed ω_r were considered to be constant.

The value of the reference rotor flux magnitude is obtained from the reference flux calculator as function of the power factor PF_ref and electromagnetic torque reference value T_{e_ref}.

The torque and flux hysteresis comparators provide logical output that is used together with $\hat{\psi}_{r\_x}$ and $\hat{\psi}_{r\_y}$ for switching pattern establishment defined by an optimal switching table.

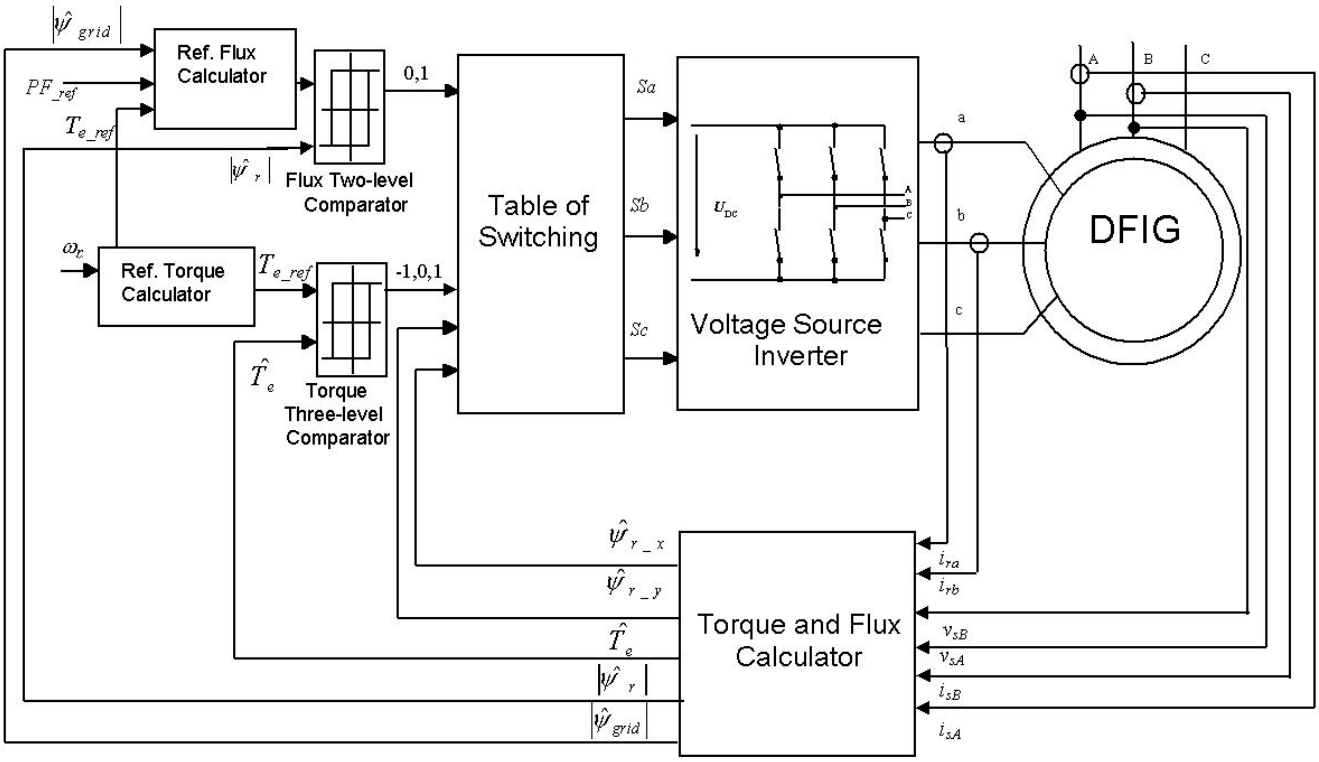

Fig. 2. The Block structure of the modified DTC control of the doubly fed wind-power induction generator

When the switching pattern is established, a voltage phasor is applied to the rotor and this voltage will change the rotor flux. The tangential component of the voltage vector controls the torque whereas the radial component increases or decreases the flux magnitude.

IV. CROWBAR

The crowbar circuit that was used in simulations consists of a diode bridge that rectifies the rotor phase currents and a single thyristor in series with resistance R_{crow} as it is depicted in Fig. 3.

The crowbar doesn't work in chopper mode. The thyristor is turned on when the DC link voltage U_{dc} reaches its maximum value

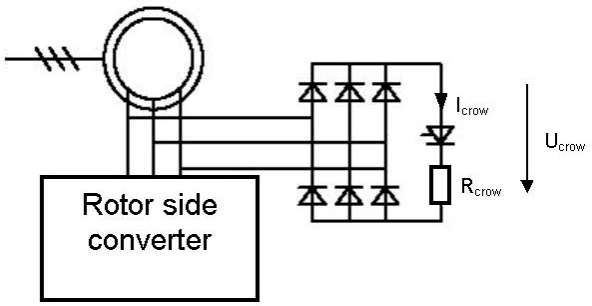

Fig. 3. Diode bridge crowbar

$$U_{dc} \geq U_{dc\max} \tag{15}$$

Simultaneously the rotor circuit is disconnected from the rotor side frequency converter and connected to the crowbar. The rotor remains connected to the crowbar until the main circuit breaker disconnects the stator from the network.

The rectified current I_{crow} can be calculated from DFIG rotor currents as

$$I_{crow} = (|i_{ra}| - i_{ra} + |i_{rb}| - i_{rb} + |i_{rc}| - i_{rc})/2 \tag{16}$$

The dc voltage over the crowbar U_{crow} is calculated as

$$U_{crow} = R_{crow} I_{crow} - U_{CB\_semic} \tag{17}$$

where $U_{CB\,semic}$ denotes the voltage drop over the thyristor.

V. MODELING OF THE NETWORK, TRANSFORMER AND TRANSMISSION LINE

The network represents the simple model with a three-phase voltage source in series with a short circuit inductance and reactance.

The transmission line between the network and the transformer is modeled with its resistance, inductance and capacitance by π-equivalent circuit.

The transformer model contains a short circuit resistance and inductance and stray capacitance of the winding. The transformer is considered to be linear, i.e. magnetic saturation has not been taken into account.

VI. Simulation Results

The analysis was carried out in Matlab – Simulink simulation environment. The fixed simulation time-step was set to 0.5e-7 and forward Euler method was used.

The operation of the 1.7 MVA DFIG before and during the fault in the network was investigated by applying constant torque T_{ref} = – 0.5 p.u. at the constant speed 1.0667 p.u., which represents a half-power operational condition a of DFIG with the amplitudes of the stator and rotor currents being about 0.5 p.u in steady state.

The simulation results are presented in per-unit system with the base values corresponding to the amplitudes of the respective quantities V_{base} = 563 V, I_{base} = 2.03 kA, T_{base} = 10.9 kNm.

A. Simulation of DFIG under network disturbances without crowbar

The 3-phase short circuit has been introduced at time instant 5 s. The fault has been modeled by a stator voltage reduction down to 35% of the nominal value.

The transient stator current, rotor current and electromagnetic torque when the crowbar is not implemented are depicted in Fig. 4, and in detail in Fig 5. Fig. 6 shows the detailed stator, rotor and DC-link voltage waveforms.

Due to the resulting high transient currents in the rotor with a peak value more than 3.5 p.u., the DC link voltage rises up and the protection disconnects the rotor from the DC link by turning off all positive side IGBTs and turning on all negative side IGBTs thus short circuiting the rotor. A high transient current can also be observed at the stator side and its amplitude is a bit less than 2 p.u.

The electromagnetic torque due to the transients in the rotor and stator first increases in negative direction down to –1.8 p.u., then rapidly rises in the positive direction up to 1.6 p.u. and then starts to oscillate. At the time instance 5.3 s, the stator of DFIG is disconnected from the network by opening the main circuit breaker because the network fault remains.

B. Simulation of DFIG under network disturbances with the crowbar

Similarly as in previous case the 3-phase short circuit has been introduced at the time instant 5 s and fault has been modeled by a stator voltage reduction down to 35% of the nominal value. The diode bridge crowbar has been modeled according to the description in the previous chapter.

The simulated transient stator current, rotor current and electromagnetic torque, when the crowbar over-current protection is implemented are depicted in Fig. 7, and in detail in Fig 8. Fig. 9 shows the detailed stator, rotor and DC-link voltages during the fault in the network when the crowbar is turned on. The crowbar dc voltage U_{crow} and crowbar current I_{crow} are depicted in Fig. 10.

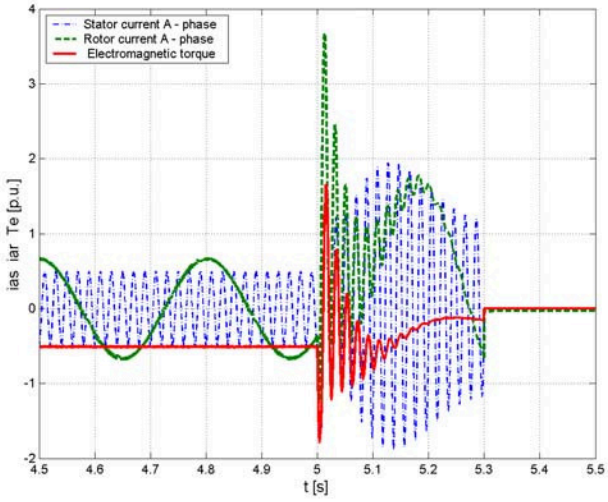

Fig. 4. Stator current (dash dot), rotor current (dash) and electromagnetic torque (solid) during network disturbance without the crowbar.

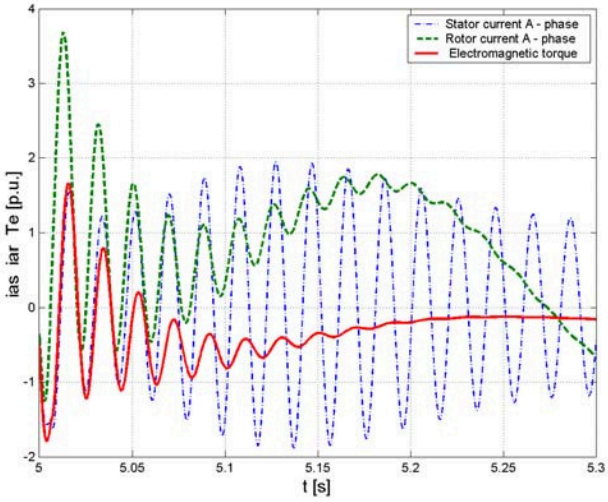

Fig. 5. Stator current (dash dot), rotor current (dash) and electromagnetic torque (solid) during network disturbance without the crowbar.

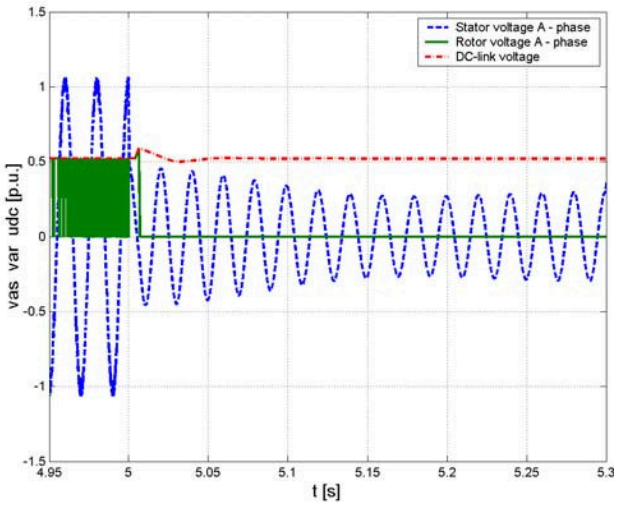

Fig. 6. Stator voltage (dash), rotor voltage (solid) and DC-link voltage (dash dot) during network disturbance without the crowbar.

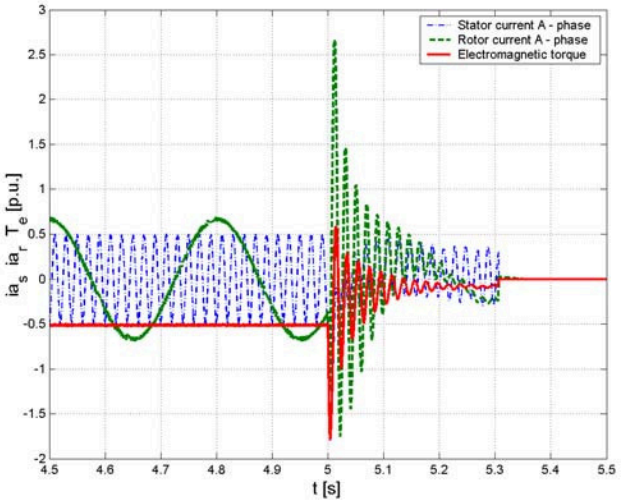

Fig. 7. Stator current (dash dot), rotor current (dash) and electromagnetic torque (solid) during network disturbance with the crowbar implemented.

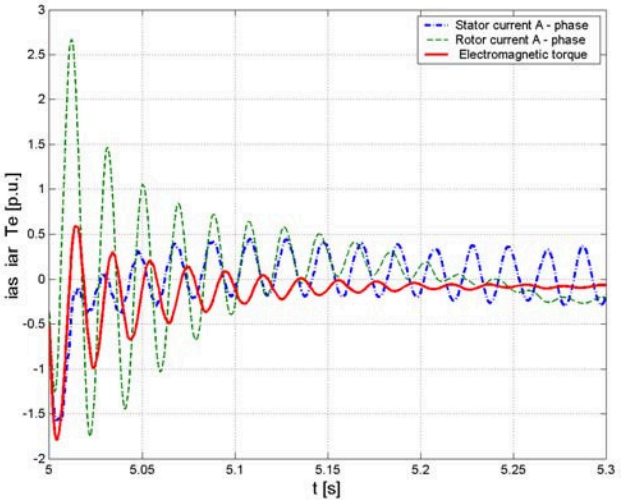

Fig. 8. Stator current (dash dot), rotor current (dash) and electromagnetic torque (solid) during network disturbance with the crowbar implemented.

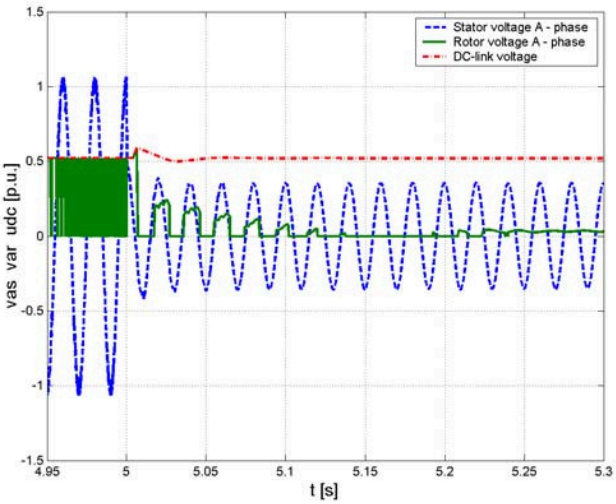

Fig. 9. Stator voltage (dash), rotor voltage (solid) and DC-link voltage (dash dot) during network disturbance with the crowbar implemented.

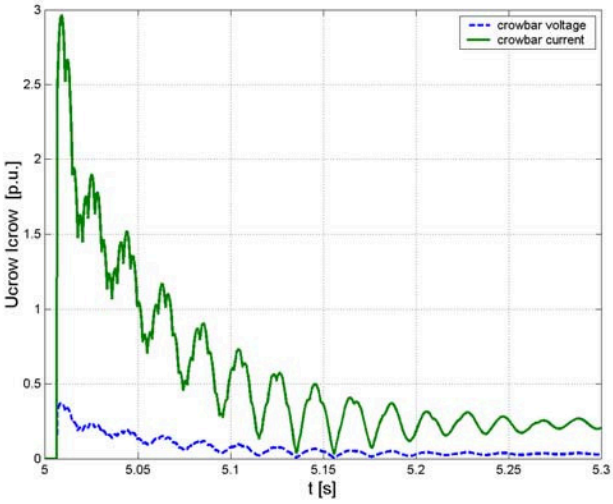

Fig. 10. Crowbar voltage (dashed) and current (solid).

The high transient currents in the rotor with a peak value more than 2.7 p.u. causes an increase of the DC-link voltage and the protection disconnects the rotor from the frequency converter.

At the same time, the rotor circuit is connected to the crowbar by turning on the crowbar thyristor. The high transient current rapidly decays down to 0.5 p.u. In comparison with the previous case the electromagnetic torque first increases in negative direction and then rapidly in the positive direction up to 1.6 p.u. and then starts to oscillate. The oscillation lasts for 0.2 s and at the steady state the torque is almost zero. The stator is disconnected from the network at the time instance 5.3 s by opening the main circuit breaker.

VII. Conclusions

Transient behavior of a doubly fed wind-power induction generator connected to the network and controlled by modified direct torque control has been studied. The transient simulation results of a 1.7 MVA DFIG under a three-phase network short circuit with and without crowbar have been compared. Comparison shows that when the crowbar is implemented, the stator and rotor transient current decay rapidly to value with amplitude lower than 1 p.u and rotor circuit is properly protected. Simulation results also show that the amplitude of transient electromagnetic torque is reduced when the crowbar is activated. On the other hand the electromagnetic torque oscillates longer than in case without crowbar. Simulink analytical model of the DFIG together with control that have been developed and tested are suitable for including in large simulation structure including a wind turbine model when the voltage dip due to symmetrical network fault ride through is studied.

REFERENCES

[1] J. B. Ekanayake, L. Holdsworth, X. G. Wu, N. Jenkins, "Dynamic Modeling of Doubly Fed Induction Generator Wind Turbines," *IEEE Transaction on Power Systems,* Vol. 18. No. 2, May 2003, pp. 803 – 809.

[2] J. G. Slootweg, H. Polinder, W. L.Kling, "Dynamic Modeling of a Wind Turbine with Doubly Fed Induction Generator " *Proc. of 2001 IEEE Power Engineering Society Summer Meeting*, Vol. 1, pp. 644 – 649.

[3] L. Holdsworth, X. G. Wu; J. B. Ekanayake, N. Jenkins: "Comparison of fixed speed and doubly-fed induction wind turbines during power system disturbances" *IEE Proceedings - Generation, Transmission and Distribution*, Volume: 150, Issue: 3, 13 May 2003, pp. 343 – 352.

[4] A. Tapia, G. Tapia, J.X. Ostolaza, J. R. Saenz: "Modeling and control of a wind turbine driven doubly fed induction generator" *IEEE Transactions on Energy Conversion,* Volume: 18, Issue: 2, June 2003, pp. 194 – 204.

[5] R. Koessler, S Pillutla, L. Trinh, D. Dickmander: "Integration of large wind farms into utility grids (Part 1 - Modeling of DFIG)", *Proc. of 2003 IEEE PES General Meeting*.

[6] M. H. J. Bollen, M. Martins, G. Olguin, "Voltage dips at the terminals of wind-power installations," presented at the Nordic Wind Power Conference 2004, 1-2 March 2004, Chalmers University of Technology, Göteborg, Sweden.

[7] F. Runcos, R. Carlson, A. M. Oliveira, P. Kuo-Peng, N. Sadowski, "Performance Analysis of a Brushless Double Fed Cage Induction Generator," presented at the Nordic Wind Power Conference 2004, 1-2 March 2004, Chalmers University of Technology, Göteborg, Sweden.

[8] A. Petersson, S. Lundberg, T. Thiringer, "A DFIG Wind-trubine Ride-Through System Influence on the Energy Production," presented at the Nordic Wind Power Conference 2004, 1-2 March 2004, Chalmers University of Technology, Göteborg, Sweden.

[9] J. Niiranen, "Voltage Dip Ride Through of Doubly-fed Generator Equipped with Active Crowbar, " presented at the Nordic Wind Power Conference 2004, 1-2 March 2004, Chalmers University of Technology, Göteborg, Sweden.

[10] S. Arnalte, J. C. Burgos, J. L. Rodrigues-Amenedo: "Direct Torque Control of a Doubly-Fed Induction Generator for Variable Speed Wind Turbines", *Electric Power Components and Systems*, No. 30, 2002, pp. 199-216.